



OPEN Carbonate mineral precipitation induced by microorganisms enriched from the cave water and biofilm in a lime-decorated lava tube

Yumi Kim¹, Sung-min Kang¹, Kyoung-nam Jo² & Yul Roh¹✉

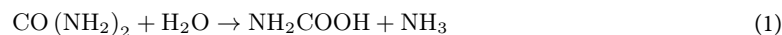
Cave microorganisms associated with calcareous speleothems have been reported to facilitate calcium carbonate precipitation through crystal nucleation and mineral growth. In this study, we used carbonate-forming microorganisms enriched from cave water droplets and stalactite biofilm samples to induce precipitation of Mg^{2+} or Sr^{2+} -coprecipitated carbonate minerals and explored their mineralogical properties. The samples for these analyses were collected from Yongcheon Cave, a lime-decorated lava tube located on Jeju Island in South Korea. They included five soil and sediment samples from outside the cave, seven drip water samples from inside the cave, and nine biofilm samples swiped using sterilized cotton swabs from inside the cave. The microorganisms enriched from the drip water samples comprised bacterial genera, including *Pseudomonas*, *Bacillus*, *Stenotrophomonas*, *Acinetobacter*, and *Morganella*, which are known to contribute to carbonate formation. In contrast, the microorganisms enriched from the biofilms were dominated by *Pseudomonas*. When only Ca^{2+} was present in the growth medium ($\text{Ca}:\text{Sr} = 3:0$), these microorganisms precipitated calcite and vaterite. Conversely, when Ca^{2+} and Sr^{2+} were present at varying ratios ($\text{Ca}:\text{Sr} = 2:1$, $1:1$, and $1:2$), calcian-strontianite was precipitated. Furthermore, when only Sr^{2+} was present ($\text{Ca}:\text{Sr} = 0:3$), strontianite was formed. Adding Ca^{2+} and Mg^{2+} at varying ratios ($\text{Ca}:\text{Mg} = 2:1$, $1:1$, and $1:2$) led to the precipitation of magnesian-calcite and monohydrocalcite. When only Mg^{2+} was added to the medium ($\text{Ca}:\text{Mg} = 0:3$), nesquehonite and struvite precipitated. These findings suggest that microorganisms enriched from the lava tube cave induce calcium carbonate precipitation through ureolysis and that Sr/Ca and Mg/Ca ratios influence the type of precipitated carbonate or phosphate minerals.

Keywords Cave, Microorganisms, Calcium carbonate, Sr, Mg, Biomineralization, MICP

Carbonate compounds are derived from the combination of the carbonate anion complex (CO_3^{2-}) with cations such as Ca^{2+} , Mg^{2+} , Fe^{2+} , Sr^{2+} , or rare earth elements. Carbonate precipitation is a common natural phenomenon in environments such as seawater, freshwater, soil, and sediments. Carbonates in the form of limestone and dolomite are the major carbon reservoirs on Earth, storing approximately 42% of the total carbon¹, and most of these carbonate minerals are known to be of biological origin from bacteria, fungi, and algae^{2,11}. Therefore, the study of microbially induced calcium carbonate precipitation (MICP) is not only crucial for understanding the environment of cation and carbon fixation through microbial metabolism in nature but also has immense potential as an eco-friendly method for the development of biomaterial synthesis and engineering application technologies and ecological conservation^{3,4,11}. To date, the most widely studied bacterial mechanism for calcium carbonate precipitation is the ureolytic metabolic pathway. This process begins with the production of carbamate (NH_2COOH) by microbial urease, followed by its spontaneous hydrolysis into ammonia (NH_3) and carbonic acid (H_2CO_3) (see Eqs. 1, 2). These products then react with water (H_2O) to form carbonate (CO_3^{2-}), ammonium (NH_4^+), and hydroxyl ions (OH^-), ultimately raising the pH of the surrounding medium (see Eqs. 3, 4)^{5,6}. Then,

¹Department of Geological and Environmental Sciences, Chonnam National University, 77 Yongbong-Ro, Buk-Gu, Gwangju 61186, Republic of Korea. ²Department of Geology, Kangwon National University, Chuncheon 24341, Republic of Korea. ✉email: rohy@jnu.ac.kr

the dissolved calcium ion (Ca^{2+}) combines with the carbonate to precipitate calcium carbonate (CaCO_3) (see Eq. 5).



In alkaline environments, Ca^{2+} ions and bacterial cells, acting as nucleation sites, facilitate the precipitation of calcium carbonate^{7–9}. Among the bacteria involved in this process, *Sporosarcina pasteurii* is well known for its ability to precipitate calcium carbonate through active ureolysis. However, another pathway, carbonic anhydrase, has been implicated in MICP and CO_2 sequestration. Carbonic anhydrase is a zinc-containing metalloenzyme that catalyzes the reversible hydration of CO_2 into bicarbonate and hydrogen ions. Under alkaline conditions, HCO_3^- can interact with Ca^{2+} ions and precipitate as calcium carbonate¹⁰. Additionally, various microbial metabolic pathways, including photosynthesis, denitrification, and redox conditions, can influence bacterial calcification in nature¹¹. Moreover, MICP research has extended beyond the study of polymorphic calcium carbonates (e.g. calcite, aragonite, vaterite) to examine the effects of other cations on the coprecipitation or precipitation of carbonate minerals in calcium carbonate. For instance, previous studies have demonstrated that the precipitation of heavy metals (e.g., Cd^{2+} , Pb^{2+} , Cu^{2+}) and radionuclides (e.g., Sr^{2+}) through MICP can serve as a promising method for contaminant removal¹². Furthermore, they have emphasized that understanding the interactions with other abundant cations in the Earth's crust (e.g., Mg^{2+}) offers valuable insights into the geochemical metal cycle.

Caves, typically isolated and oligotrophic environments with no light, offer favorable conditions for microorganisms owing to their high humidity levels and stable temperatures. Urea originates from mammalian urine (e.g., human, pig, cow etc.) or chemical fertilizers around caves. When it infiltrates into the cave environment, it can induce carbonate mineral precipitation by ureolytic microorganisms living inside the cave^{13–17}. To date, studies have reported numerous microbes participating in MICP to form crystalline secondary cave deposits, known as speleothems¹⁸. These microbes are also known to play a role in promoting the nucleation and growth of calcium carbonate crystals¹⁹.

Yongcheon Cave, is a lava cave located on Jeju Island, and formed by several lava flows during the late Quaternary period. Inside the cave, carbonate speleothems such as soda straws, stalactites, and stalagmites are found throughout the passages. A previous study traced paleoclimate changes through the trace element ratios of Mg, Sr, and P in the stalagmites of this cave. Mg and Sr originate from carbonate minerals in wind-blown marine sediments outside the cave surface, while P can be supplied from organic matter in the soil. The study reported that the Mg/Ca, Sr/Ca, and P/Ca ratios of Yongcheon Cave stalagmites increased in the mid- to late-nineteenth century due to intensified dissolution in the weathered zone, caused by increased temperature and precipitation²⁰. Although these elemental ratios are attributed to chemical precipitation from groundwater, their specific effects on the microbially induced precipitation of carbonate minerals are yet to be explored. To bridge this gap, the current study aimed to examine calcium carbonate precipitation by microorganisms enriched from drip water and stalagmite biofilm samples sourced from Yongcheon Cave. It also aimed to evaluate the influence of Sr/Ca and Mg/Ca ratios on the formation of the resulting carbonate minerals.

Results and discussion

Geochemical and mineralogical characteristics of the surface sediments

In the dune sediments collected from the surface of cave, mostly marine organism shells such as foraminifera and a small amount of volcanic rock fragments were observed (Fig. S1). The minerals of the sediments were mainly magnesian-calcite [$(\text{Ca}, \text{Mg})\text{CO}_3$] and aragonite (CaCO_3), and the soils mainly contained quartz and magnesian-calcite (Fig. S2). Therefore, the component contents of the sediments were in the order of CaO (86.2%), MgO (4.2%), SiO_2 (4.9%), and Al_2O_3 (2.3%), while the soil samples were in the order of CaO (40.5%), SiO_2 (35.7%), Al_2O_3 (11.1%), and MgO (3.4%). The organic acid contents were analyzed as isobutyric acid ($\text{C}_4\text{H}_8\text{O}_2$) in the dune sediments and soils, with an average of 55.5 mg/L and 109.0 mg/L, respectively (Table S1). As previously reported²¹, the calcareous dune sediments and soils covering the cave surface provided an environment in which organic acids and various cations (Ca^{2+} , Mg^{2+} , etc.) could be supplied into the cave.

Geochemical characteristics of the drip water samples

To acquire insights into the growth environment of microorganisms inhabiting Yongcheon Cave, the drip water samples were subjected to geochemical analyses. The pH values of the samples ranged from 7.9 to 8.3, with an average of 8.1, indicating a slightly alkaline environment (Table S2). The average concentrations of major ions in the drip water samples were as follows (Table S2): Ca: 50.9 mg/L, Na: 9.7 mg/L, Mg: 8.9 mg/L, K: 7.3 mg/L, and Si: 5.8 mg/L. Apart from these major ions, trace elements were also detected, including Fe (357 $\mu\text{g/L}$), Sr (313.2 $\mu\text{g/L}$), Ba (6.2 $\mu\text{g/L}$), and Al (4.1 $\mu\text{g/L}$). The concentrations of NH_4^+ in the drip water samples were mostly less than 0.1 mg/L, but was as high as 3.37 mg/L in DW 6 (Table S2). The main source of nitrogen in cave water in this study area was reported to be affected by chemical fertilizers²¹.

Diversity of carbonate-forming microorganisms in the drip water and biofilm samples

Figure 1 illustrates the microbial diversity derived from the NGS analysis of the enriched microorganisms. The results indicate that the microorganisms enriched from the drip water samples primarily comprise *Proteobacteria* (average 64.1%) and *Firmicutes* (average 31.4%) at the phylum level. The microbial diversity analysis of the communities cultured from the seven drip water samples revealed 21 bacterial genera with a relative abundance of more than 1%, including microorganisms known to induce carbonate precipitation. *Pseudomonas* was the dominant genus among the microorganisms enriched from the DW 3, DW 6, and DW 7 samples, with relative proportions of 92.6%, 60.8%, and 17.2%, respectively. Meanwhile, *Bacillus* accounted for 8.3% of the microorganisms enriched from the DW 7 sample. These microbial genera, commonly found in soil and cave environments, have previously been identified as key members of cave microbial communities^{22–24}. They are also known for their remarkable ability to induce carbonate precipitation through urease and carbon anhydrase activity¹¹. In particular, *Stenotrophomonas* sp., comprising 64.5% of the microbial community enriched from the DW 7 sample, predominantly inhabits soil environments and plays a pivotal role in CO₂ fixation by inducing carbonate precipitation via carbon anhydrase^{25,26}. Notably, the microbial communities cultured from the drip water samples primarily included genera that are commonly found in soil, such as *Pseudomonas* sp., *Bacillus* sp., and *Stenotrophomonas* sp. This indicates that the microbial population within the cave is likely influenced by the external environment^{23,27}. Previous studies have reported that *Morganella morganii*, *Pseudochrobactrum* sp., and *Brevundimonas* sp. induce calcium carbonate precipitation through urease production, while *Neisseria* sp. contributes to this process via carbon anhydrase production^{10,28–30}. These findings suggest that the internal environment of Yongcheon Cave creates favorable biogeochemical conditions for carbonate mineral precipitation.

Among the microorganisms enriched from the nine biofilm samples, *Proteobacteria* was the dominant phylum, with an average abundance of 94%. In these samples, 21 bacterial genera with a relative abundance of over 1% were identified, with *Pseudomonas* sp. being dominant in all biofilm samples except for BF 3 and BF 5. Microorganisms known to participate in carbonate mineral precipitation, such as *Proteus* sp., *Stenotrophomonas* sp., *Bacillus* sp., *Pseudochrobactrum* sp., *Acinetobacter* sp., and *Brevundimonas* sp., were also identified^{24,28–31}. Among these, *Acinetobacter* sp. has been isolated from caves and is known to be involved in biofilm formation associated with speleothems and calcite precipitation³². Previous studies have also demonstrated that *Pseudomonas* sp. and *Morganella morganii* can form biofilms through the secretion of extracellular polymeric substances (EPSs)^{33,34}. Notably, the EPSs produced by microorganisms contain negatively charged functional

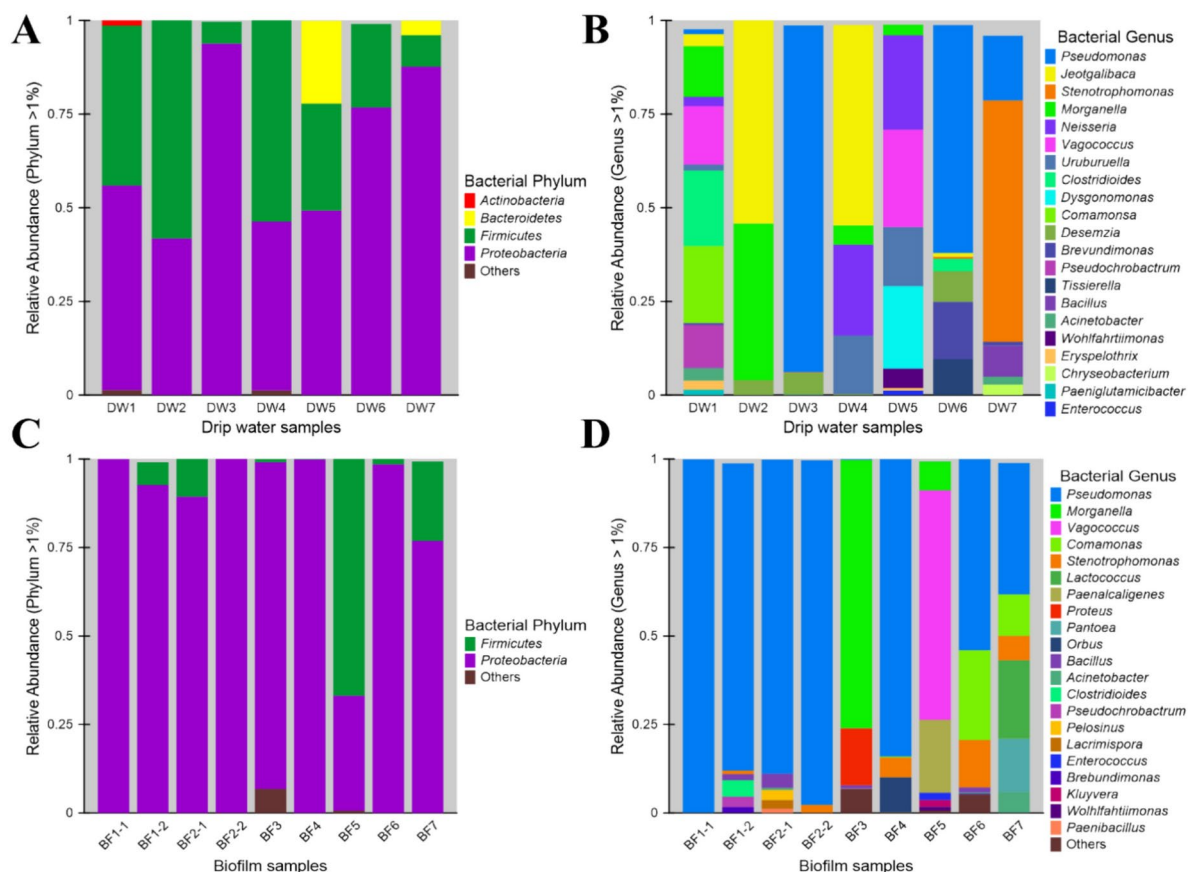


Fig. 1. Microbial diversity results of microorganisms enriched from the drip water and biofilm samples, derived from the NGS analysis.

groups, such as carboxyl, phosphate, amine, and hydroxyl groups, which are known to adsorb various divalent cations (Ca^{2+} , Mg^{2+} , and Sr^{2+}), facilitating mineral nucleation and calcium carbonate precipitation¹¹.

Microbially induced calcium carbonate precipitation

For the next phase of our analysis, microorganisms enriched from the drip water and biofilm samples were inoculated into media containing urea and 0.03 mol/L CaCl_2 and subsequently cultured at 15 °C. Within 48 h, changes in turbidity owing to microbial growth were observed (Fig. S3). White precipitates formed under all experimental conditions within 5 days and were subsequently recovered after 1 week. XRD analysis confirmed that these precipitates predominantly contained calcite (Fig. S4). Among the cultures, those enriched from the drip water sample DW 5 and biofilm sample BF 1–2, which demonstrated relatively fast precipitation rates (within 48 h), were selected for further experiments to explore the effects of Mg/Ca and Sr/Ca ratios on carbonate mineral formation.

Effect of Mg/Ca ratios on carbonate precipitation

Our next analysis delved into the effects of various Ca^{2+} and Mg^{2+} content ratios (Ca:Mg = 3:0, 2:1, 1:1, 1:2, and 0:3) on carbonate mineral formation by *S. pasteurii* and the microorganisms cultured from the DW 5 and BF 1–2 samples. Across all experimental conditions, the initial pH increased from 7.00 to between 9.36 and 9.51 after one week. This increase was attributed to the formation of OH^- ions during microbial growth and urea decomposition (Fig. S5). While solution turbidity and precipitation rate changed more gradually with increasing Mg^{2+} content, similar outcomes were observed across all conditions after 7 days.

ICP-MS analysis revealed that more than 99% of Ca^{2+} was removed on average under all experimental conditions, confirming that microbial growth induced calcium carbonate precipitation (Table S5). In contrast, the concentration of Mg^{2+} was reduced by only 12.2–58.6% compared to the initial concentration, indicating that only a small fraction of Mg^{2+} was converted to a mineral. Among the three tested microorganisms, *S. pasteurii*, known for its calcium-carbonate-forming ability, demonstrated the lowest Mg^{2+} removal efficiency.

Figure 2 illustrates the results of the XRD analysis conducted to identify the mineral precipitates formed by the three microorganisms. Notably, when only Ca^{2+} was present in the medium (Ca:Mg = 3:0), calcium carbonate minerals such as calcite and vaterite formed. At Ca:Mg ratios of 2:1 and 1:2, carbonate minerals such as magnesian-calcite and monohydrocalcite ($\text{CaCO}_3 \cdot \text{H}_2\text{O}$), as well as magnesium ammonium phosphate compounds such as struvite $[(\text{NH}_4)\text{Mg}(\text{PO}_4) \cdot 6\text{H}_2\text{O}]$, precipitated. When only Mg^{2+} was present (Ca:Mg = 0:3), magnesium ammonium phosphate compounds such as struvite and dittmarite $[(\text{NH}_4)\text{Mg}(\text{PO}_4) \cdot \text{H}_2\text{O}]$, along with nesquehonite ($\text{MgCO}_3 \cdot 3\text{H}_2\text{O}$), a magnesium carbonate mineral, were formed.

The morphologies of the precipitated minerals were observed using SEM-EDS (Fig. 3, Table S5). Notably, the calcite particles formed at a Ca:Mg ratio of 3:0 appeared as spherical particles with diameters of approximately 30–40 μm (Fig. 3A). High magnification observations revealed that these particles were covered with smaller rhombohedral particles, measuring approximately 2–3 μm in length (Fig. 3B), and their compositions included Ca, C, and O (Fig. 3C). Furthermore, magnesian-calcite, precipitated at a Ca:Mg ratio of 2:1, appeared as spherical particles with diameters of approximately 20–30 μm , and the surfaces of these particles were covered with rhombohedral particles measuring 0.2–0.3 μm in length. These particles contained Ca, Mg, C, and O (Fig. 3F). The minerals formed by the microorganisms cultured from BF 1–2 exhibited cell-sized pores, suggesting microbial involvement in precipitation (Fig. 3D,E). Meanwhile, the precipitates formed at a Ca:Mg ratio of 0:3 comprised Mg, P, and O and manifested as plate-shaped particles that aggregated into a columnar structure with a length of approximately 30 μm (Fig. 3G–I). Therefore, Mg^{2+} did not coprecipitate with calcium

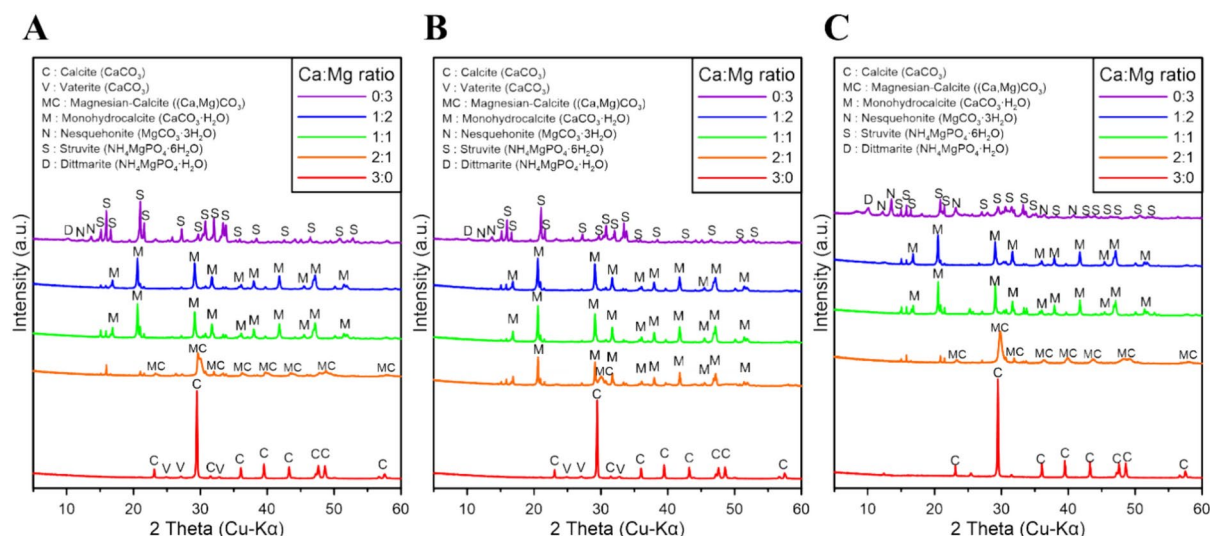


Fig. 2. XRD spectra of minerals precipitated by *S. pasteurii* (A) and the microbial communities cultured from DW 5 (B) and BF 1–2 (C) at varying Ca:Mg ratios in the medium.

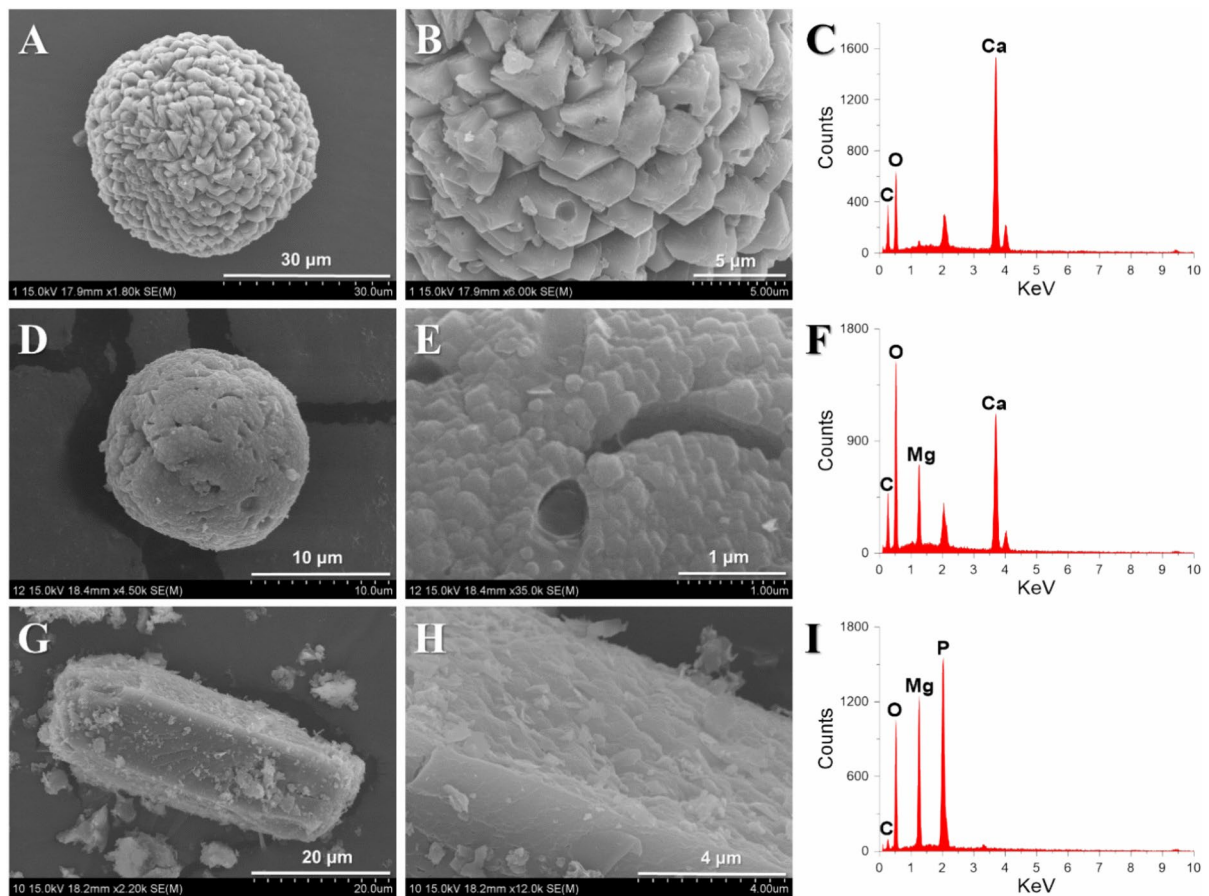


Fig. 3. SEM-EDS analysis of minerals formed at varying Ca:Mg ratios in the growth medium: calcium carbonate (A–C) formed at Ca:Mg = 3:0 by *S. pasteurii*, magnesian-calcite (D–F) formed at Ca:Mg = 2:1 by the microorganisms cultured from BF 1–2, and magnesium ammonium phosphate (G–I) formed at Ca:Mg = 0:3 by the microorganisms cultured from DW 5.

carbonate for Mg/Ca ratios of one and above. However, at Mg/Ca ratios below one, magnesian-calcite, with Mg^{2+} incorporated into its structure, was formed. Furthermore, when only Mg^{2+} was present, it tended to precipitate as struvite, a phosphate mineral, rather than as nesquehonite, a carbonate mineral.

Effect of Sr/Ca ratios on carbonate precipitation

Our next analysis focused on examining the effects of various Ca^{2+} and Sr^{2+} content ratios (Ca:Sr = 3:0, 2:1, 1:1, 1:2, and 0:3) on carbonate mineral formation by the species enriched from samples DW 5 and BF 1–2 and *S. pasteurii*. Under all experimental conditions, the turbidity of the medium increased within 24 h of microbial inoculation, and white precipitates formed within 48 h. The ureolytic bacterium *S. pasteurii* raised the pH of the medium from 7.0 to approximately 8.4 within the first 24 h of cultivation, achieving a maximum pH of 9.6 on day 9 (Fig. S5). Similarly, the microbial species enriched from the DW 5 and BF 1–2 samples also gradually elevated pH values, reaching a maximum of 9.5 on day 9 (Fig. S5). However, the rate of pH increase was slower for the species enriched from the DW 5 sample. This increase in pH indicates that urea hydrolysis occurred during microbial growth. Examinations of the changes in Ca^{2+} and Sr^{2+} concentrations revealed that *S. pasteurii* achieved high removal efficiency, with average removal rates of 99.6% for Ca and 99.9% for Sr^{2+} , regardless of the Sr/Ca ratio. This Sr^{2+} removal rate is similar to the findings of previous experiments utilizing *S. pasteurii*¹¹. Furthermore, in the medium inoculated with microorganisms enriched from the DW 5 and BF 1–2 samples, the average Ca^{2+} removal rates were 96.7% and 99.4%, while the average Sr^{2+} removal rates were 99.2% and 99.9%, respectively, regardless of the Sr/Ca ratio (Table S6). These findings suggest that both Ca^{2+} and Sr^{2+} ions in the medium transformed into solid precipitates owing to microbial activity.

When only Ca^{2+} was present in the medium (Ca:Sr = 3:0), calcite precipitated as spherical particles with diameters of approximately 40–50 µm length (Figs. 4 and 5A,B). These particles were made up of Ca, C, and O, and their surfaces were covered with rhombohedral particles 1–2 µm in length (Fig. 5B,C). At a Ca:Sr ratio of 2:1, a mixture of calcian-strontianite [(Ca,Sr) CO_3] and calcite precipitated, with calcian-strontianite forming spherical particles. These particles, measuring 10–20 µm in diameter, were composed of needle-like structures (Fig. 5D–F). As the Sr^{2+} content increased (Ca:Sr = 1:1 and 1:2), calcian-strontianite continued to precipitate as spherical particles with diameters of approximately 10–20 µm, maintaining needle-like structures.

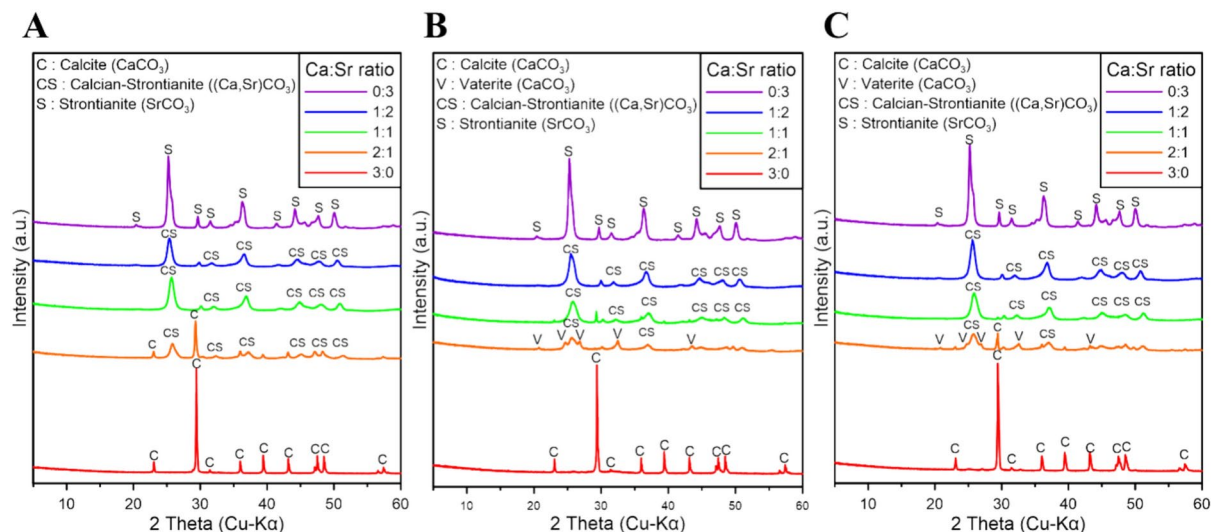


Fig. 4. XRD spectra of minerals precipitated by *S. pasteurii* (A) and the microbial communities cultured from the DW 5 (B) and BF 1–2 (C) samples at varying Ca:Sr ratios in the medium.

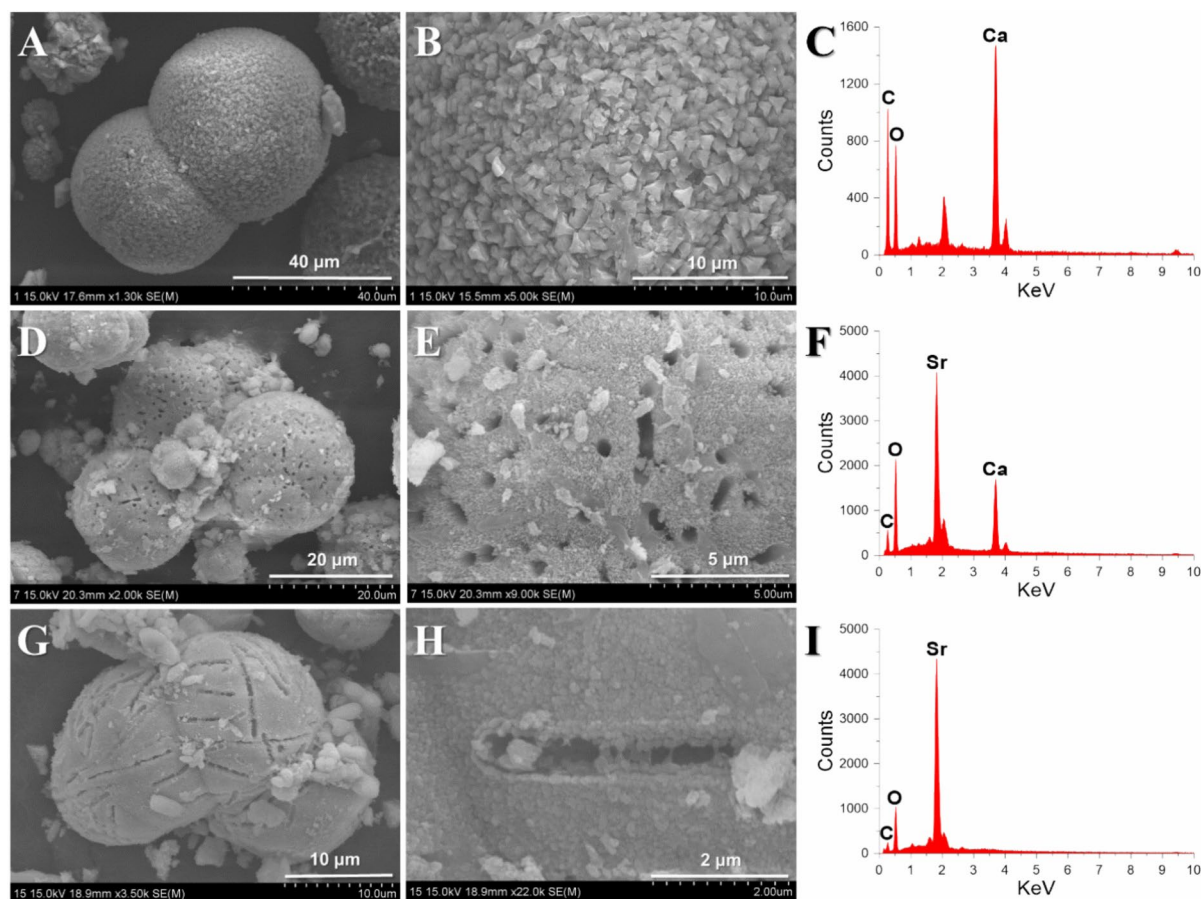


Fig. 5. SEM-EDS analysis of minerals formed at varying Ca:Sr ratios in the growth medium: CaCO_3 (A–C) formed at Ca:Sr = 3:0 by *S. pasteurii*, calcian-strontianite (D–F) formed at Ca:Sr = 2:1 by the microorganisms in DW5, and strontianite (G–I) formed at Ca:Sr = 0:3 by the microorganisms in BF1–2.

However, at Ca:Sr = 1:1, calcian-strontianite predominantly formed irregular particles, with some needle-like particles aggregating into spheres exhibiting diameters of 5–10 μm . When only Sr^{2+} was present in the medium (Ca:Sr = 0:3), strontianite (SrCO_3), a pure Sr carbonate mineral, precipitated as block-like or spherical particles with diameters of approximately 40–50 μm and rough surfaces (Fig. 5G–I). In the XRD pattern, the d -spacing of the (111) face of calcian-strontianite, formed by the three microorganisms, tended to increase with rising Sr^{2+} content (Fig. 5 and Table S6). This indicates that Sr, featuring a larger ionic radius (ionic radius = 0.113 nm) compared to Ca (ionic radius = 0.099 nm), replaced Ca in the crystal structures of calcian-strontianite and strontianite^{35,36}.

Regardless of the microorganism type, minerals precipitated in the presence of only Ca^{2+} or Sr^{2+} (Ca:Sr = 3:0 and 0:3) displayed distinct peaks in the XRD spectra and appeared as spherical particles with diameters of approximately 40–50 μm in the SEM-EDS analysis. Conversely, minerals precipitated in the combined presence of Ca^{2+} and Sr^{2+} (Ca:Sr = 2:1, 1:1, and 1:2) displayed broad peaks in the XRD spectra and appeared as irregular or spherical particles with diameters of approximately 5–20 μm in the SEM-EDS analysis. This indicates that minerals precipitated solely in the presence of Ca^{2+} or Sr^{2+} exhibit higher crystallinity and larger particle sizes compared to those formed in the combined presence of both Ca^{2+} and Sr^{2+} . Although Ca^{2+} and Sr^{2+} share similar chemical properties, their physical and chemical differences hinder the growth of carbonate mineral crystals³⁷. This inference aligns with the results of previous research demonstrating that Sr^{2+} competes with Ca^{2+} for adsorption at carbonate mineral growth sites, leading to a decrease in mineral growth rates³⁸. Our study also demonstrates that the crystallinity and sizes of precipitated mineral particles vary with the Sr/Ca ratio. In our previous study, adding $\text{SrCl}_2 \cdot 6\text{H}_2\text{O}$ at different ratios to a medium containing 0.03 mol/L $\text{CaCl}_2 \cdot 2\text{H}_2\text{O}$ confirmed that when the Sr/Ca ratio was below one, Sr^{2+} tended to coprecipitate with calcium carbonate. Conversely, when the Sr/Ca ratio exceeded 1, Ca tended to coprecipitate with strontianite¹². At Sr/Ca ratios below 1, the precipitated minerals displayed characteristics typical of calcium carbonate forms, such as calcite, aragonite, and vaterite, alongside calcian-strontianite. In our experiment, similar mineral characteristics were observed even as the Sr/Ca concentration ratio was altered within the total cation concentration limit of 0.03 mol/L. At Ca:Sr = 2:1, where calcian-strontianite began to form, *S. pasteurii* induced calcite precipitation, while the microbial communities cultured from the DW 5 and BF 1–2 samples induced vaterite precipitation (Fig. 4). Further analysis revealed elongated, rod-shaped holes and traces, which are bacterial imprints in the carbonate minerals precipitated by the microbial communities cultured from the DW 5 and BF 1–2 samples (Fig. 5D,G). In particular, the microbial community cultured from the BF 1–2 sample presented traces and holes (Fig. 5D–F), likely formed through the calcification of microorganisms. This suggests a close relationship between microbial EPS formation and carbonate mineral precipitation.

Therefore, the reason why Sr^{2+} could be more easily incorporated into calcite than Mg^{2+} during microbially induced calcium carbonate precipitation may be because the chemical binding and hydration energies of Sr^{2+} are less than that of Ca^{2+} , but the binding and hydration energies of Mg^{2+} are greater than that of Ca^{2+} ³⁷.

Materials and methods

Yongcheon Cave

Yongcheon Cave, located on Jeju Island, South Korea, is a typical lava cave formed by multiple lava flows during the late Quaternary period. This cave features diverse carbonate speleothems, including popcorn, soda straws, stalactites, and stalagmites, which are scattered throughout its passageways³⁹. For this study, drip water and microbial biofilm samples were collected from this cave. Notably, the speleothems of Yongcheon Cave are believed to form through abiotic (chemical) pathways, creating calcareous crystals owing to interactions between humic acid from the soil and Ca from overlying calcareous dunes³⁹.

The dune has been formed by wind-driven movement of beach sediments composed of biogenic carbonate sediments (approx. 95%) and volcanic rock fragments including detrital minerals (approx. 5%)⁴⁰. The temperature inside the cave is 15.5–21.3 °C, and the water temperature is 15–16.5 °C, maintaining a stable environment all year round⁴¹.

Collection of sediments, drip water and biofilm samples

For the experiment, two dune sediment samples and three soil samples were collected from five different locations outside the cave to investigate the mineralogical and chemical composition of the sediments overlying the lava tube (Fig. S6). Water dripping from stalactites and soda straws on the cave ceiling was sampled at seven different locations (Fig. 6). This drip water was added to 50 mL conical tubes, sealed, and stored at 4 °C in a refrigerator before incubation. Additionally, nine biofilm samples were collected by swabbing the surfaces of speleothems and the inner walls of the containers used to collect the drip water (Table 1). Sterile cotton swabs were used for this purpose, and the swabs were immediately transferred to 15 mL conical tubes containing 2 mL of a growth medium. These tubes were also stored at 4 °C until further use.

Cultivation of carbonate-forming microorganisms from the drip water and biofilm samples

To enrich the carbonate-forming microorganisms present in the collected drip water and biofilm samples, a modified growth medium containing 10 g/L yeast extract, 5 g/L proteose peptone, 1 g/L glucose, and 5 g/L NaCl was utilized^{11,42,43}. This medium was autoclaved at 121 °C and 1.2 kgf/cm² for 20 min, with an initial pH of approximately 6.6. To induce calcium carbonate precipitation following microbial urea decomposition, 20 g/L urea and 0.03 mol/L calcium chloride ($\text{CaCl}_2 \cdot 2\text{H}_2\text{O}$) were added to the medium using a 0.2 μm filter^{11,42,43}. For the enrichment of carbonate-forming microorganisms in the drip water samples, 10 mL of drip water was injected into 50 mL of the liquid medium containing urea and calcium chloride. This mixture was then allowed to stand in an aerobic environment at 15 °C for 7 days. Meanwhile, for the microbial enrichment of the biofilm samples, 0.5 mL of the biofilm-mixed medium was added to 50 mL of the liquid medium.

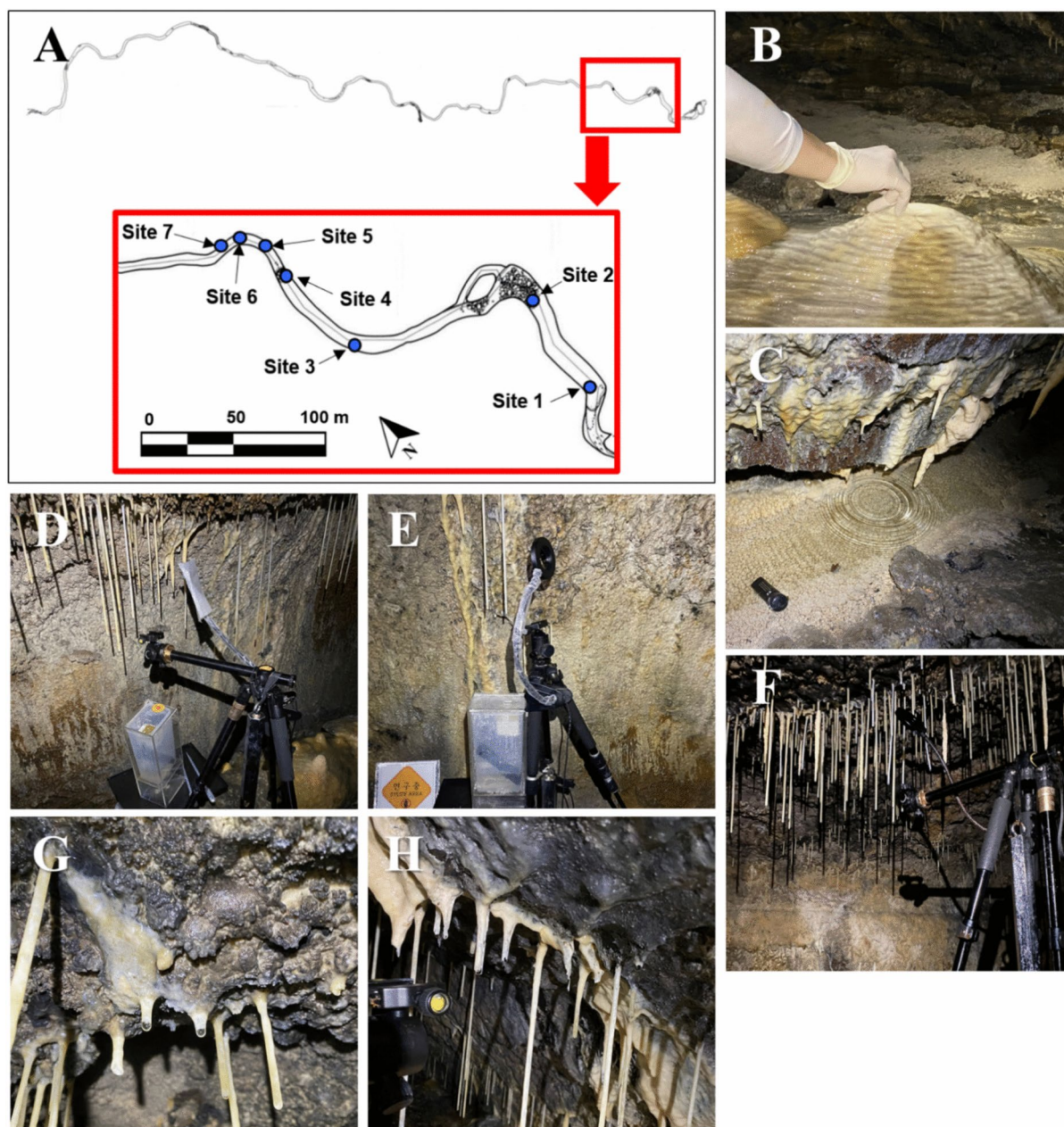


Fig. 6. Drip water and biofilm sampling sites within the cave (A: cave map; B: site 1; C: site 2; D: site 3; E: site 4; F: site 5; G: site 6; and H: site 7).

Effects of Mg/Ca and Sr/Ca ratios on microbially induced calcium carbonate precipitation

To investigate the effects of Sr/Ca and Mg/Ca ratios on microbially induced calcium carbonate precipitation, stock solutions of Ca, Sr, and Mg were prepared. For this, 1 M solutions of calcium chloride ($\text{CaCl}_2 \cdot 2\text{H}_2\text{O}$, molecular weight (MW): 147.01), magnesium chloride (MgCl_2 , MW: 95.21), and strontium chloride hexahydrate ($\text{SrCl}_2 \cdot 6\text{H}_2\text{O}$, MW: 266.62) separately added to distilled water and autoclaved. Previous studies^{11,43} have reported the addition of a 0.03 mol/L Ca solution to the medium to initiate microbially induced calcium carbonate precipitation. Based on this, in our experiment, the total cation concentration in the medium was maintained at 0.03 mol/L, while the Mg/Ca and Sr/Ca ratios were varied as follows: Ca:Mg and Ca:Sr = 3:0, 2:1, 1:1, 1:2, and 0:3. Subsequently, the effects of these ratios on carbonate mineral formation were examined using the microorganism strains enriched from drip water sample DW 5 and biofilm sample BF 1–2. For comparison, *S. pasteurii* KCTC 3558, a strain known for its excellent calcium carbonate precipitation ability, was used as the reference.

To induce calcium carbonate precipitation via microbial ureolysis, 1 mL of the microbial cultures (1% v/v) were added to 100 mL of urea-containing media with varying Sr/Ca and Mg/Ca ratios. The cultures were then incubated at 15 °C for 14 days to allow mineral precipitation. During the experiment, 5 mL of suspension was withdrawn using a syringe on days 1, 3, 7, and 14 to monitor changes in pH and cation concentrations (Ca^{2+} ,

Sampling sites	Drip water	Biofilm	
	Samples	Samples	Description
1	DW 1	BF 1-1	Water container wall
		BF 1-2	Stalagmite surface
2	DW 2	BF 2-1	Stalactite surface
		BF 2-2	Water chemistry measuring rod surface
3	DW 3	BF 3	Water container wall
4	DW 4	BF 4	Water container wall
5	DW 5	BF 5	Water container wall
6	DW 6	BF 6	Water container wall
7	DW 7	BF 7	Water container wall

Table 1. Drip water and biofilm samples collected for microbial enrichment.

Sr²⁺, and Mg²⁺) in the supernatant. Furthermore, the mineralogical properties of the precipitates recovered from the samples were analyzed.

Analytical methods

To investigate the mineralogy and geochemistry of dune sediments (S1–S2) and soil samples (S3–S5) covering the cave, X-ray diffraction (XRD) and X-ray fluorescence analysis (XRF) were performed using an Empyrean 3D high-resolution X-ray diffractometer (Malvern Panalytical, Malvern, U.K.) equipped with a Cu-Kα radiation source (40 kV, 30 mA, 0.06°/s) and a XRF-1800 equipment (SHIMADZU, Japan), respectively. Organic acid content of sediment and soil samples was measured by high performance liquid chromatography (HPLC) analysis using Prominence HPLC equipment (SHIMADZU, Japan).

To investigate the characteristics of the microbial communities, second-generation cultures, subcultured from the initial enriched cultures, were examined using next-generation sequencing (NGS). For the NGS analysis, 10 mL of the microbial cultures were centrifuged for one week, forming a pellet. These pellets were then analyzed using MACROGEN.

To acquire insights into the geochemical environment of the cave, the pH of the drip water samples (DW 1–DW 7) was measured, and their chemical composition was analyzed using inductively coupled plasma-atomic emission spectroscopy (ICP-AES) and inductively coupled plasma-mass spectrometry (ICP-MS) with a Nexion 2000 system (Perkin-Elmer, Waltham MA, USA), following standard methods. During the experiments on microbially induced carbonate precipitation, changes in Ca²⁺, Sr²⁺, and Mg²⁺ concentrations in the medium were recorded at the start (day 0) and after 14 days using ICP-AES analysis. Ammonium (NH₄⁺) concentrations were determined using Nessler's method with an HI97715 Ammonia Medium Range Photometer from Hanna Instruments⁴⁴. For all analyses, the culture media were centrifuged at 3500 rpm for 10 min, and the resulting supernatant was filtered through a 0.45 μm syringe filter. The supernatant was then diluted 1000 times with distilled water before testing.

To analyze the mineralogical characteristics of the precipitates formed by the microorganisms, X-ray diffraction (XRD) and field-emission scanning electron microscopy (FE-SEM) coupled with energy-dispersive X-ray spectroscopy (EDS) were utilized. The samples for the XRD and SEM analyses were prepared by centrifuging the suspension at 3000 rpm for 5 min. After removing the supernatant, the remaining residue was rinsed twice with distilled water and subsequently dried in an oven at 60 °C overnight to obtain solid precipitates. XRD was conducted using the same process as the sediment analysis described above. Meanwhile, the FE-SEM analysis, aimed at examining the morphology and elemental composition of the precipitates, was performed using a Hitachi S-4700 FE-SE microscope (Hitachi, Tokyo, Japan) at an accelerating voltage of 15–20 kV, coupled with an EDS instrument (Phillips, Eindhoven, Netherlands).

Conclusion

Carbonate-forming microorganisms were enriched and cultured from drip water and biofilm samples collected from Yongcheon Cave. Microbial diversity analysis confirmed the presence of several microorganisms capable of inducing calcium carbonate precipitation, including *Pseudomonas* sp., *Bacillus* sp., *Stenotrophomonas* sp., *Acinetobacter* sp., and *Morganella* sp. Previous studies have demonstrated that these microorganisms not only create favorable chemical conditions for calcium carbonate precipitation through urease and carbon anhydrase activity but also promote carbonate mineral precipitation through EPS formation. In the current study, microorganisms enriched from the drip water and biofilm samples effectively transformed ionized Ca species within urea-containing media into calcium carbonate. When Ca²⁺ and Sr²⁺ were mixed at varying ratios, calcian-strontianite—a form of calcium carbonate coprecipitated with Ca²⁺ and Sr²⁺—was formed. Notably, Sr²⁺ exhibited high efficiency of carbonate mineral precipitation, comparable to that of Ca²⁺, regardless of its content ratio. In contrast, Mg²⁺ demonstrated low efficiency of mineral precipitation. When only Mg²⁺ was present in the medium, the microorganisms tended to precipitate phosphate minerals, such as struvite and dittmarite, instead of carbonate minerals. The microorganisms cultured from the DW 5 and BF 1–2 samples exhibited high Sr²⁺ removal efficiency, similar to *S. pasteurii*, forming carbonate minerals in Sr-containing media. However, their Mg²⁺ removal efficiency in Mg-containing media surpassed that of *S. pasteurii*. These findings indicate that the indigenous microorganisms within the lime-decorated lava tube can induce the precipitation of various minerals

when divalent cations such as Ca^{2+} , Mg^{2+} , and Sr^{2+} are present in different ratios in drip water or sediments, contributing to geochemical cycles. Furthermore, the formation of carbonate minerals through microbial activity presents a promising environmentally friendly approach for the immobilization of radioactive isotopes (e.g., ^{90}Sr) and the potential sequestration of carbon dioxide in natural environments.

Data availability

Data is provided within the manuscript or supplementary information files.

Received: 3 December 2024; Accepted: 21 February 2025

Published online: 28 February 2025

References

- Ehrlich, H. L. *Geomicrobiology* (Marcel Dekker, 1996).
- Jones, B. Review of calcium carbonate polymorph precipitation in spring systems. *Sediment. Geol.* **353**, 64–75. <https://doi.org/10.1016/j.sedgeo.2017.03.006> (2017).
- Jimoh, O. A., Okoye, P. U., Ariffin, K. S., Hussin, H. B. & Baharun, N. Continuous synthesis of precipitated calcium carbonate using a tubular reactor with the aid of aloe vera (*Aloe barbadensis* Miller) extract as a green morphological modifier. *J. Clean. Prod.* **150**, 104–111. <https://doi.org/10.1016/j.jclepro.2017.02.200> (2017).
- Zhang, C. et al. Contribution of selective bacterial extracellular polymeric substances to the polymorphism and morphologies of formed Ca/Mg carbonates. *Int. Biodeterior. Biodegrad.* **160**, 105213. <https://doi.org/10.1016/j.ibiod.2021.105213> (2021).
- Ronca, S. et al. Biogenic calcium carbonate as evidence for life. *Biogeosciences* **20**, 4135–4145. <https://doi.org/10.5194/bg-20-4135-2023> (2023).
- Mitchell, A. C. et al. Kinetics of calcite precipitation by ureolytic bacteria under aerobic and anaerobic conditions. *Biogeosciences* **16**, 2147–2161. <https://doi.org/10.5194/bg-16-2147-2019> (2019).
- Stocks-Fischer, S., Galinat, J. K. & Bang, S. S. Microbiological precipitation of CaCO_3 . *Soil Biol. Biochem.* **31**, 1563–1571. [https://doi.org/10.1016/S0038-0717\(99\)00082-6](https://doi.org/10.1016/S0038-0717(99)00082-6) (1999).
- Ferris, F. G., Phoenix, V., Fujita, Y. & Smith, R. W. Kinetics of calcite precipitation induced by ureolytic bacteria at 10 to 20 °C in artificial groundwater. *Geochim. Cosmochim. Acta* **67**(8), 1701–1710. [https://doi.org/10.1016/S0016-7037\(03\)00503-9](https://doi.org/10.1016/S0016-7037(03)00503-9) (2003).
- Omeregbe, A. I., Palombo, E. A. & Nissom, P. M. Bioprecipitation of calcium carbonate mediated by ureolysis: A review. *Environ. Eng. Res.* **26**, 200379. <https://doi.org/10.4491/eeer.2020.379> (2021).
- Boone, C. D., Gill, S., Habibzadegan, A. & McKenna, R. Carbonic anhydrase: An efficient enzyme with possible global implications. *Int. J. Chem. Eng.* **2013**, 813931. <https://doi.org/10.1155/2013/813931> (2013).
- Zhu, T. & Dittrich, M. Carbonate precipitation through microbial activities in natural environment, and their potential in biotechnology: A review. *Front. Bioeng. Biotechnol.* **4**, 4. <https://doi.org/10.3389/fbioe.2016.00004> (2016).
- Kim, Y., Kwon, S. & Roh, Y. Effect of divalent cations (Cu, Zn, Pb, Cd, and Sr) on microbially induced calcium carbonate precipitation and mineralogical properties. *Front. Microbiol.* **12**, 646748. <https://doi.org/10.3389/fmicb.2021.646748> (2021).
- Johnston, M. D., Muench, B. A., Banks, E. D. & Barton, H. A. Human urine in Lechuguilla Cave: The microbiological impact and potential for bioremediation. *J. Caves Karst Stud.* **74**, 278–291. <https://doi.org/10.4311/2011MB0227> (2012).
- Chen, H. J., Huang, Y. H., Chen, C. C., Maity, J. P. & Chen, C. Y. Microbial induced calcium carbonate precipitation (MICP) using pig urine as an alternative to industrial urea. *Waste Biomass Valor.* **10**, 2887–2895. <https://doi.org/10.1007/s12649-018-0324-8> (2019).
- Comadran-Casas, C., Schaschke, C. J., Akunna, J. C. & Jorat, M. E. Cow urine as a source of nutrients for Microbial-Induced Calcite Precipitation in sandy soil. *J. Environ. Manage.* **304**, 114307. <https://doi.org/10.1016/j.jenvman.2021.114307> (2022).
- Gowthaman, S., Koizumi, H., Nakashima, K. & Kawasaki, S. Field experimentation of bio-cementation using low-cost cementation media for preservation of slope surface. *Case Stud. Constr. Mater.* **18**, e02086. <https://doi.org/10.1016/j.cscm.2023.e02086> (2023).
- Ortiz, M. et al. Profiling bacterial diversity and taxonomic composition on speleothem surfaces in Kartchner Caverns. *AZ. Microb. Ecol.* **65**, 371–383. <https://doi.org/10.1007/s00248-012-0143-6> (2013).
- Koning, K. et al. Biomineralization in cave bacteria—Popcorn and soda straw crystal formations, morphologies, and potential metabolic pathways. *Front. Microbiol.* **13**, 933388. <https://doi.org/10.3389/fmicb.2022.933388> (2022).
- Banks, E. D. et al. Bacterial calcium carbonate precipitation in cave environments: A function of calcium homeostasis. *Geomicrobiol. J.* **27**(5), 444–454. <https://doi.org/10.1080/01490450903485136> (2010).
- Woo, K. S., Jo, K., Yi, S., Yang, D. Y. & Li, H. C. Paleoclimatic investigation using trace elemental compositions of the YC-1 stalagmite, Yongcheon Cave, Jeju Island, Korea for the past 600 years. *J. Geol. Soc. Korea* **49**(3), 325–337. <https://doi.org/10.14770/jgsk.2013.49.3.325> (2013).
- Research and Investigation on Jeju Island Natural Cave Conservation and Management Plan (No. 79-6500655-000040-14), Jeju Special Self-Governing Province, 2020, p. 45 (written in Korean).
- Busquets, A., Fornós, J. J., Zafra, F., Lalucat, J. & Merino, A. Microbial communities in a coastal cave: Cova des Pas de Vallgornera (Mallorca, Western Mediterranean). *Int. J. Speleol.* **43**(2), 205–216. <https://doi.org/10.5038/1827-806X.43.2.8> (2014).
- Park, S., Cho, Y. J., Jung, D. Y., Lee, E. J. & Lee, J. S. Microbial diversity in moonmilk of Baeg-nyong Cave, Korean CZO. *Front. Microbiol.* **11**, 511189. <https://doi.org/10.3389/fmicb.2020.00613> (2020).
- Jurado, V. et al. Microbial communities in carbonate precipitates from drip waters in Nerja Cave, Spain. *PeerJ* **10**, e13399. <https://doi.org/10.7717/peerj.13399> (2022).
- Okuy, T. O., Nguyen, H. N., Castro, S. L. & Rodrigues, D. F. CO_2 sequestration by ureolytic microbial consortia through microbially-induced calcite precipitation. *Sci. Total Environ.* **572**, 671–680. <https://doi.org/10.1016/j.scitotenv.2016.06.199> (2016).
- Enyedi, N. T. et al. Cave bacteria-induced amorphous calcium carbonate formation. *Sci. Rep.* **10**(1), 8696. <https://doi.org/10.1038/s41598-020-65667-w> (2020).
- Wu, Y., Tan, L., Liu, W. & Wang, J. Profiling bacterial diversity in a limestone cave of the western Loess Plateau of China. *Front. Microbiol.* **6**, 130020. <https://doi.org/10.3389/fmicb.2015.00244> (2015).
- Mukherjee, S., Sahu, R. B., Mukherjee, J. & Sadhu, S. Application of microbial-induced carbonate precipitation for soil improvement via ureolysis. *Ground Improv. Tech. Geosynth.* **2**, 85–94. https://doi.org/10.1007/978-981-13-0559-7_10 (2019).
- Ali, A. et al. *Brevundimonas diminuta* isolated from mines polluted soil immobilized cadmium (Cd^{2+}) and zinc (Zn^{2+}) through calcium carbonate precipitation: Microscopic and spectroscopic investigations. *Sci. Total Environ.* **813**, 152668. <https://doi.org/10.1016/j.scitotenv.2021.152668> (2022).
- Sheng, M. et al. Micro-dynamic process of cadmium removal by microbial induced carbonate precipitation. *Environ. Pollut.* **308**, 119585. <https://doi.org/10.1016/j.envpol.2022.119585> (2022).
- Kang, S. & Roh, Y. Biomineralization of Mg-enriched calcium carbonates by aerobic microorganisms enriched from rhodoliths. *J. Nanosci. Nanotechnol.* **17**(4), 2329–2332. <https://doi.org/10.1166/jnn.2017.13316> (2017).
- Banerjee, S. & Joshi, S. R. Ultrastructural analysis of calcite crystal patterns formed by biofilm bacteria associated with cave speleothems. *J. Microsc. Ultrastruct.* **2**(4), 217–223. <https://doi.org/10.1016/j.jmau.2014.06.001> (2014).

33. Li, X. et al. Spatial patterns of carbonate biomineralization in biofilms. *Appl. Environ. Microbiol.* **81**(21), 7403–7410. <https://doi.org/10.1128/AEM.01585-15> (2015).
34. Müller, A. R., Leite, B. R. & Corção, G. Analysis of antibiotic resistance and biofilm-forming capacity in tetracycline-resistant bacteria from a coastal lagoon. *Microb. Drug Resist.* **28**(6), 654–659. <https://doi.org/10.1089/mdr.2021.0255> (2022).
35. Finch, A. A. & Allison, N. Coordination of Sr and Mg in calcite and aragonite. *Mineral. Mag.* **71**(5), 539–552. <https://doi.org/10.1180/minmag.2007.071.5.539> (2007).
36. Tovani, C. B., Oliveira, T. M., Gloter, A. & Ramos, A. P. Sr²⁺-substituted CaCO₃ nanorods: Impact on the structure and bioactivity. *Cryst. Growth Des.* **18**(5), 2932–2940. <https://doi.org/10.1021/acs.cgd.8b00017> (2018).
37. Knight, A. W. et al. The combined effects of Mg²⁺ and Sr²⁺ incorporation during CaCO₃ precipitation and crystal growth. *Geochim. Cosmochim. Acta* **345**, 16–33. <https://doi.org/10.1016/j.gca.2023.01.021> (2023).
38. Mitchell, A. C. & Ferris, F. G. Effect of strontium contaminants upon the size and solubility of calcite crystals precipitated by the bacterial hydrolysis of urea. *Environ. Sci. Technol.* **40**(3), 1008–1014. <https://doi.org/10.1021/es050929p> (2006).
39. Woo, K. S. et al. Geological heritage values of the Yongcheon Cave (lava tube cave), Jeju Island, Korea. *Geoheritage* **11**(2), 615–628. <https://doi.org/10.1007/s12371-018-0315-y> (2019).
40. Woo, K. S. et al. The origin of erratic calcite speleothem in the Dangcheomul Cave (lava tube cave), Jeju Island, Korea. *Quat. Int.* **70–81**, 176–177. <https://doi.org/10.1016/j.quaint.2007.05.009> (2008).
41. Ji, H. S., Woo, K. S. & Yang, D. Y. Little Ice Age recorded in the YC-2 stalagmite of the Yongcheon Cave, Jeju Island (South Korea). *Korean Meteorol. Society* **20**, 261–271 (2010) (in Korean with English abstract).
42. Sánchez-Román, M., Vasconcelos, C., Warthmann, R., Rivadeneyra, M. & McKenzie, J. A. Microbial dolomite precipitation under aerobic conditions: Results from Brejo do Espinho Lagoon (Brazil) and culture experiments. *Perspect. Carbonate Geol. Tribute Career Robert Nathan Ginsburg* **41**, 167–178. <https://doi.org/10.1002/9781444312065.ch11> (2009).
43. Kim, Y. & Roh, Y. Microbially induced carbonate precipitation using microorganisms enriched from calcareous materials in marine environments and their metabolites. *Minerals* **9**, 722. <https://doi.org/10.3390/min9120722> (2019).
44. Dikshit, R., Jain, A., Dey, A. & Kumar, A. Microbially induced calcite precipitation using *Bacillus velezensis* with guar gum. *PLoS ONE* **15**(8), e0236745. <https://doi.org/10.1371/journal.pone.0236745> (2020).

Acknowledgements

This research was supported by the National Research Foundation of Korea (NRF-2022R1C1C2009540 and 2022R1A2C1005449). We extend our sincere gratitude to the researchers at the Earth Paleoenvironment Lab of Kangwon National University for their assistance with drip water and biofilm sampling and the CCRF and CDFC of Chonnam National University in Gwangju and Yeosu, as well as the KBSI- Gwangju center, for their valuable analytical support.

Author contributions

First author, YK: Conceptualization, Methodology, Formal analysis, Investigation, Writing—Preparation of the Original Manuscript, SK: Data curation, Formal analysis, Investigation, Writing—Preparation of the Original Manuscript, KJ: Resources, YR: Supervision, Conceptualization, Methodology, Funding acquisition, Writing—Reviewing and Editing of the Original Manuscript.

Declarations

Competing interests

The authors declare no competing interests.

Additional information

Supplementary Information The online version contains supplementary material available at <https://doi.org/10.1038/s41598-025-91585-w>.

Correspondence and requests for materials should be addressed to Y.R.

Reprints and permissions information is available at www.nature.com/reprints.

Publisher's note Springer Nature remains neutral with regard to jurisdictional claims in published maps and institutional affiliations.

Open Access This article is licensed under a Creative Commons Attribution-NonCommercial-NoDerivatives 4.0 International License, which permits any non-commercial use, sharing, distribution and reproduction in any medium or format, as long as you give appropriate credit to the original author(s) and the source, provide a link to the Creative Commons licence, and indicate if you modified the licensed material. You do not have permission under this licence to share adapted material derived from this article or parts of it. The images or other third party material in this article are included in the article's Creative Commons licence, unless indicated otherwise in a credit line to the material. If material is not included in the article's Creative Commons licence and your intended use is not permitted by statutory regulation or exceeds the permitted use, you will need to obtain permission directly from the copyright holder. To view a copy of this licence, visit <http://creativecommons.org/licenses/by-nc-nd/4.0/>.

© The Author(s) 2025